JACS
JOURNAL OF THE AMERICAN CHEMICAL SOCIETY

Article

pubs.acs.org/JACS

Analyzing Structure–Photophysical Property Relationships for Isolated T_8, T_{10}, and T_{12} Stilbenevinylsilsesquioxanes

Joseph C. Furgal,[†] Jae Hwan Jung,[§] Theodore Goodson, III,*[,†,§] and Richard M. Laine*[,‡,§]

[†]Department of Chemistry, [‡]Materials Science and Engineering, and [§]Macromolecular Science and Engineering, University of Michigan, Ann Arbor, Michigan 48109-2136, United States

Supporting Information

ABSTRACT: Silsesquioxanes (SQs) are of considerable interest for hybrid electronic and photonic materials. However, to date, their photophysical properties have not been studied extensively, thus their potential remains conjecture. Here we describe the first known efforts to map structure–photophysical properties as a function of cage symmetry and size by comparing identically functionalized systems. Our focus here is on the solution photophysical properties of the title stilbenevinyl-SQs, which were characterized using single photon absorption, two-photon absorption, fluorescence emission, and fluorescence lifetime kinetics. We offer here the first detailed photophysical study of the larger pure T_{10} and T_{12} silsesquioxanes and show photophysical properties that differ as a function of size, especially in their fluorescence behavior, indicating that cage size and/or symmetry can strongly affect photophysical properties. We also find that they offer excitation-dependent emission (evidence of rare "red-edge" effects). The T_{10} stilbenevinyl-SQ offers up to a 10-fold increase in two-photon absorption cross section per chromophore over a free chromophore, signifying increased electronic coupling. The SQ cage compounds show "rise times" of 700–1000 fs and low anisotropy (~0.1) in fluorescence lifetime kinetic studies. These results indicate excited state energy transfer, unobserved for the free chromophores and unexpected for systems with "inert" silica cores and for 3-D hybrid molecular species. These findings provide the first detailed photophysical study of chromophore-functionalized T_{10} and T_{12} silsesquioxanes and show that SQs may be considered a separate class of compounds/materials with anticipated novel properties of value in developing new components for electronic and photonic applications.

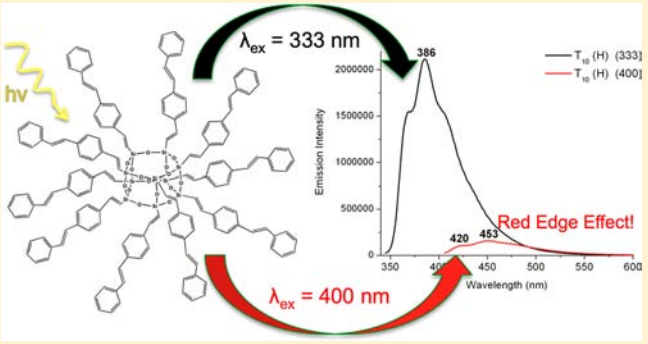

INTRODUCTION

Silsesquioxanes (SQs) are of considerable interest for hybrid electronic and photonic materials applications.[1−4] They have gained recent attention due to their unique 3-D oriented functional groups,[5−8] potential for high degrees of functionalization,[9−15] and high thermal stabilities deriving from the heat capacity of the silica core.[15,16] SQs functionalized with conjugated organic groups offer high absorption, unexpected emissive properties, tunable band gaps, and charge delocalization.[3,4,9,17,18] Until recently, most work on SQs focused on the T_8 compounds, with more than 17 reviews on the subject, with minimal emphasis given to the T_{10} and T_{12} compounds described herein.[3,12,14,19−32]

To date, very little work has targeted mapping the photophysical properties of SQs as a function of structure and symmetry, let alone cage sizes. In part, this is because the synthetic tools and separation methods that allow the synthesis and isolation of well-defined compounds were not sufficiently refined. We report here the development of both synthesis and separation methods that provide access to the pure, individual, stilbenevinyl-SQ cage compounds.[4,9,15,17,33] Strong motivation for the current work arises because their photophysical behavior often differs considerably from pure organics. Thus, there is considerable potential to develop SQs with entirely different photonic/electronic properties of potential value for multiple applications as alternatives to organic components currently in commercial use or being considered for commercial use.

Most review articles to date give little attention to the larger cages; see Figure 1. Indeed, very few studies of the larger cage systems have been reported.[9,14,19,33−35] Recently, facile access to the T_{10} and T_{12} cages was occasioned by the discovery of F^--catalyzed rearrangement of T_8 cages, T-resins, or directly from $RSi(OEt)_3$.[9,33−35] This method allows isolation in high purity of the higher cage compounds after a simple 2 day reaction, though usually as a mixture of cage sizes.

F^- catalysis offers a distinct advantage over the slow syntheses (weeks) and low yields (5–30%) reported for many T_8 cages.[3,12,23,30,36,37] Thus, our current efforts focused on isolating larger cage sizes and thereafter mapping their respective properties.[9,33]

Received: May 7, 2013
Published: July 22, 2013

   dx.doi.org/10.1021/ja4043092 | J. Am. Chem. Soc. 2013, 135, 12259–12269

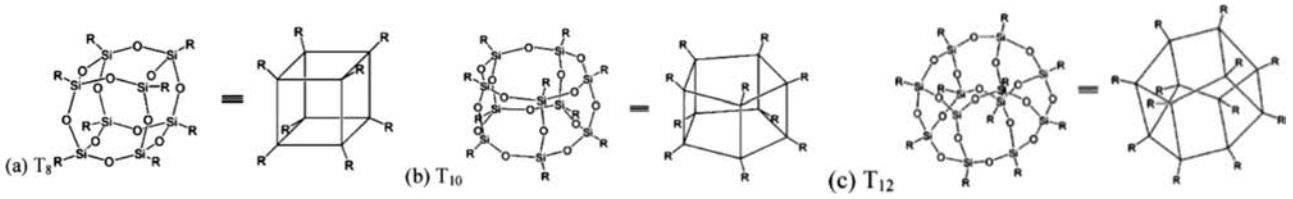

Figure 1. Examples of SQ cages and simplified structures.

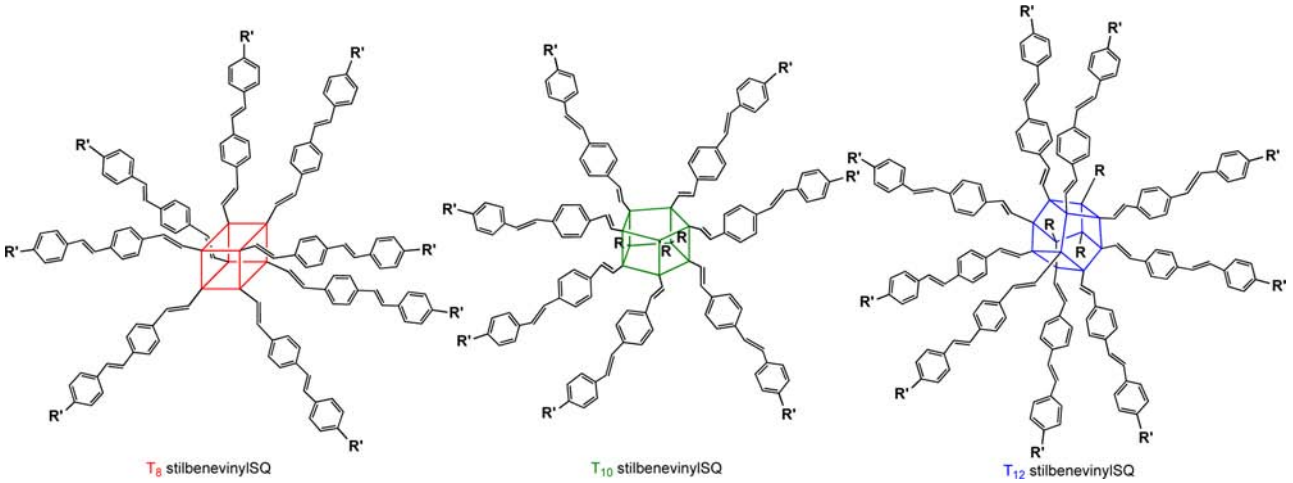

Figure 2. Stilbenevinyl-SQ cages, R = stilbenevinyl, R′ = H.

The few reports that discuss the separation of T_{10} and T_{12} SQs typically discuss their removal (as byproducts) during the purification of T_8 SQs.[5,14,30,38] Thus, we report here the synthesis, purification, and detailed studies of the photophysical properties of the model systems *p*-R-stilbenevinyl T_8, T_{10}, and T_{12} SQs. The first paper in this series developed a synthetic approach to mixed $T_{10/12}$ *p*-R-stilbenevinyl-SQs and mapped their basic photophysical properties in solution. Since our previous study looked at cage mixtures, we sought to ascertain the properties of the pure T_{10} and T_{12} *p*-R-stilbenevinyl-SQs, since the mixture offered properties that often differed from those of the T_8 *p*-R-stilbenevinyl-SQs.[9,17] Figure 2 depicts stilbenevinyl-SQs prepared and purified in the current studies. These compounds serve as models for beads on a chain (BoC) oligomer and polymer systems explored briefly below and in other papers. These same models can be considered a first step in characterizing the photophysical properties of dendronized BoCs; see the other related papers.[39,40] Finally, they also serve to provide baseline properties for the design of next generation cage systems.

The photophysical mapping efforts encompass emissive behavior, two photon absorption cross sections, fluorescence lifetime kinetics, and initial solid-state (film) studies.[41−49] These properties have not been studied extensively for any hybrid 3-D molecules, let alone SQs. In-depth studies have been done on fullerenes;[50−53] however, only simple steady-state spectroscopic studies of hybrid molecules such as carboranes are reported and show lessening conjugation on going from ortho to meta to para, as evidenced by a blue-shifting emission.[54,55]

A further objective of the work reported here was to identify properties that allow selected compounds to be designed and synthesized as possible components for hybrid photovoltaic and related photonic and electronic applications. One outcome of our design efforts is reported in a coincidentally submitted paper, where we find that rigid organic linkers provide improved 3-D conjugation.[40]

The first step in these studies used tetrabutylammonium fluoride (TBAF) catalyzed rearrangement to generate vinyl-$T_{10/12}$ mixtures. Thereafter metathesis with *p*-Br-styrene followed by Heck cross-coupling with *p*-R-styrene provided high yields of the T_{10} and T_{12} stilbenevinyl-SQs. Only at this juncture were the mixtures amenable to separation via a combination of selective precipitation and/or GPC, as discussed just below.

The isolated compounds were then characterized by MALDI-ToF, ^{29}Si NMR, steady-state spectroscopy, two-photon absorption (TPA) spectroscopy, and fluorescence lifetime kinetics. We also offer some comparison to theoretical calculations with regards to the types of interactions possible with the chromophore and cage. This overall analysis offers the first in-depth study of the photophysical properties of T_{10} and T_{12} silsesquioxanes, which can offer significant value in photonic and electronic applications due to their robust nature, absorption efficiencies, and unique 3-D symmetries.

EXPERIMENTAL SECTION

Analytical Methods. *Gel Permeation Chromatography (GPC).* All GPC analyses were done on a Waters 440 system equipped with Waters Styragel columns (7.8 × 300, HT 0.5, 2, 3, 4) with RI detection using a Waters 2410 refractometer and THF as solvent. The system was calibrated using polystyrene standards and toluene as reference. Analyses were performed using PL Caliber 7.04 software (Polymer Laboratories, Shropshire UK).

Matrix-Assisted Laser Desorption/Time-of-Flight Spectrometry. MALDI-ToF was done on a Micromass TofSpec-2E equipped with a 337 nm nitrogen laser in positive ion reflectron mode using poly(ethylene glycol) as calibration standard, dithranol as matrix, and $AgNO_3$ as ion source. Sample was prepared by mixing a solution of 5 parts matrix (10 mg/mL in THF), 5 parts sample (1 mg/mL in

dx.doi.org/10.1021/ja4043092 | J. Am. Chem. Soc. 2013, 135, 12259−12269

THF), and 1 part $AgNO_3$ (2.5 mg/mL in water) and blotting the mixture on the target plate.

NMR Analyses. All ^1H and ^{13}C NMR were run in acetone-d_6 or $CDCl_3$ on a Varian MR400 spectrometer. ^1H NMR spectra were collected at 500 MHz using a 7998.4 Hz spectral width, a relaxation delay of 0.5 s, a pulse width of 45°, 65K data points, and TMS (0.00 ppm) as an internal reference. ^{13}C NMR spectra were collected at 100 MHz using a 25 000 Hz spectral width, a relaxation delay of 1.5 s, 75K data points, a pulse width of 40°, and TMS (0.00 ppm) as the internal reference. ^{29}Si NMR spectra were obtained on a Varian vnmrs 500 MHz and were collected at 99.35 MHz using a 4960 Hz spectral width, a relaxation delay of 20 s, 4K data points, a pulse width of 7°, and TMS (0.00 ppm) as the internal reference.

Fourier-Transform Infrared Spectroscopy (FTIR). Diffuse reflectance Fourier transform (DRIFT) spectra were recorded on a Nicolet 6700 Series FTIR spectrometer (Thermo Fisher Scientific, Inc., Madison, WI). Optical grade, random cuttings of KBr (International Crystal Laboratories, Garfield, NJ) were ground, with 1.0 wt % of the sample to be analyzed. For DRIFT analyses, samples were packed firmly and leveled off at the upper edge to provide a smooth surface. The FTIR sample chamber was flushed continuously with N_2 prior to data acquisition in the range 4000−400 cm^{-1} with a precision of ±4 cm^{-1}.

Photophysical Characterization. *UV−Vis Spectrometry.* UV−vis measurements were recorded on an Agilent (model 8341) spectrophotometer in spectrophotometric grade dried THF as solvent. Concentrations were on the order of (10^{-6}−10^{-7} M), to give absorption maximum for absorption studies to about 50% for a 0.5 cm path length. Molar extinction coefficients (ε, M^{-1} cm^{-1}) were determined by plotting a standard curve with concentrations ranging from 10^{-6} to 10^{-7} M.

Photoluminescence Spectrometry. Photoluminescence measurements were obtained on a Horiba Fluoromax-2 fluorimeter in THF. The R-stilbenevinyl-SQs were studied at their respective maximum absorption wavelengths: R = H, 332 nm. Samples from UV−vis measurements were diluted to ∼10^{-7} M, in order to reduce the likelihood of excimer formation and fluorimeter detector saturation.

Solvent Comparison Studies. Samples of the R-stilbenevinyl-SQs were prepared at concentrations of ∼20 μM in THF. Then 50 μL was added to 4 mL vials and diluted to 2 mL, with various ratios of either hexanes or methanol with THF to give final concentrations of ∼1 μM. The photoluminescence was then measured for these samples and compared.

Photoluminescence Quantum Yields (Φ_{PL}). Φ_{PL} was determined by a comparison method between a standard and the sample.[56] Each sample was compared for Φ_{PL} with 1,4-bis(2-methylstyryl)benzene (Bis-MSB) at different wavelengths, in order to account for the most similar concentration between standard and sample. The solutions were diluted to three sets of concentrations with absorption ranging from 0.02 to 0.08, to reduce fluorimeter saturation and excimer formation. The total area of emission for each sample and standard was calculated by first subtracting out the background signal and then calculating the area. The experiments were repeated at least two times and were averaged. To obtain the best accuracy, the slope of a plot of emission versus absorption was determined and calculated according to the equation

$$\Phi_{PL}(x) = \left(\frac{A_s}{A_x}\right)\left(\frac{F_x}{F_s}\right)\left(\frac{n_x}{n_s}\right)^2 \Phi_{PL}(s)$$

where Φ_{PL} is the quantum yield, A is the absorption at the excitation wavelength, F is the total integrated emission, and n is the refractive index of the solution, which due to low concentration can be approximated as the refractive index of the solvent. Subscripts x and s refer to the sample and reference, respectively. These measurements may have some error due to the sensitivity of the fluorescence spectrophotometer and other environmental conditions.

Two-Photon Excited Fluorescence Measurements. To measure the two-photon absorption (TPA) cross sections, we followed the two-photon excited fluorescence (TPEF) method.[43] A 10^{-5} M solution of Coumarin 307 in methanol or Bis-MSB in cyclohexane was used as reference. The laser used for the study was a SpectraPhysics Mai Tai diode-pumped mode-locked Ti:sapphire laser. The laser wavelength was varied from 760 to 820 nm, with an average bandwidth of ∼30 nm, a ∼100 fs pulse, and 650 nm wavelengths achieved by using a SpectraPhysics OPAL and beam-doubling system pumped at 775 nm. The input power from the laser was varied by using a polarizer. An iris was placed prior to the polarizer in order to ensure a circular beam. The beam from the polarizer was focused on the sample cell (quartz cuvette, 0.5 cm path length) using a lens with a focal length of 11.5 cm. The fluorescence was collected in a direction perpendicular to the incident beam. A 1-in. focal length planoconvex lens was used to direct the collected fluorescence into a monochromator. The output from the monochromator was coupled to a photomultiplier tube. The photons were converted into counts by a photon-counting unit. A logarithmic plot between collected fluorescence photons and input intensity gave a slope of 2, ensuring a quadratic dependence between the same.[57] The intercept enabled us to calculate the TPA cross section from the action cross section by multiplying by the fluorescence quantum yield of the sample.

Fluorescence Upconversion Kinetics. The fluorescence upconversion system used in our time-resolved experiments has been described previously.[46−48] To excite our samples, a FOG-100 system (CDP) generates second-harmonic (400 nm) or third-harmonic (286 nm) light from a mode-locked Ti-sapphire laser. Polarization of the excitation beam for anisotropy measurements was controlled with a Berek compensator. All samples were held in a 1 mm thick rotating sample cuvette. Horizontally polarized fluorescence emitted from the sample was up-converted in a nonlinear crystal of β-barium borate using a pump beam at 800 nm, which first passed through a variable delay line. The instrument response function (IRF) was determined from the Raman signal of water for 400 nm excitation and standards comparison (no rise time) at 286 nm. Lifetimes were obtained by convoluting the decay profile with the instrument response function. Spectral resolution was achieved by using a monochromator and photomultiplier tube. Under the experimental conditions, the stilbenevinyl-SQ structures investigated were relatively stable, and little photodegradation was observed. MATLAB and Origin 7 were used to model the fluorescence decay profile and to calculate fluorescence lifetime kinetics.

Materials. Decavinyl- and dodecavinylsilsesquioxanes (vinyl-$T_{10/12}$) were synthesized using previously described methods or supplied by Mayaterials Inc.[9] Stilbenevinyl-$T_{10/12}$ was synthesized by previously described methods.[21] *p*-Triethoxysilylvinylstilbene (*p*-triethoxysilyl-VS) was synthesized by methods described in the Supporting Information. Methylene chloride (CH_2Cl_2) was purchased from Fisher and distilled from CaH_2 under N_2 prior to use. 1,4-Dioxane was purchased from Fisher and distilled under N_2 from Na/benzophenone prior to use. Tetrahydrofuran was purchased from Aldrich and distilled under N_2 from Na/benzophenone prior to use. All other chemicals were purchased from Fisher or Aldrich and used as received.

Separations. *General $T_{10/12}$ Cage Separation Procedure.* The stilbenevinyl-SQ cage mixture (25 mg) was added to a 5 mL test tube and dissolved with 1 mL of ethyl acetate. Acetonitrile was then added dropwise until precipitation occurred. The precipitate was then filtered using a 0.22 μm pore size syringe filter, and the solution phase was added to a new 5 mL test tube (A). The solid phase was then redissolved with THF and added to another test tube (B). To test tube A was added acetonitrile until precipitation occurred, and the process was repeated until the solution contained only stilbenevinyl-T_{10} (three or four iterations). Test tube B was dried out and redissolved in ethyl acetate, and the same procedure as that with test tube A was repeated to enrich the solid in stilbenevinyl-T_{12}. Further purification of the T_{12} was carried out using gel permeation chromatography (GPC) to give pure T_{12} for spectroscopic studies. The purity was verified by MALDI-ToF spectroscopy and silicon NMR. See the Supporting Information (Figure S1) for a visual procedure and attempted solvent systems. T_{10} stilbenevinyl-SQ: MALDI-TOF m/z (Ag^+ adduct) = 2681 [Ag-$Si_{10}O_{15}(C_{16}H_{13})_{10}$]; GPC (found) M_n = 3367; M_w = 3450; PDI = 1.02;

dx.doi.org/10.1021/ja4043092 | J. Am. Chem. Soc. 2013, 135, 12259−12269

Scheme 1. Synthesis of Stilbenevinyl-SQs

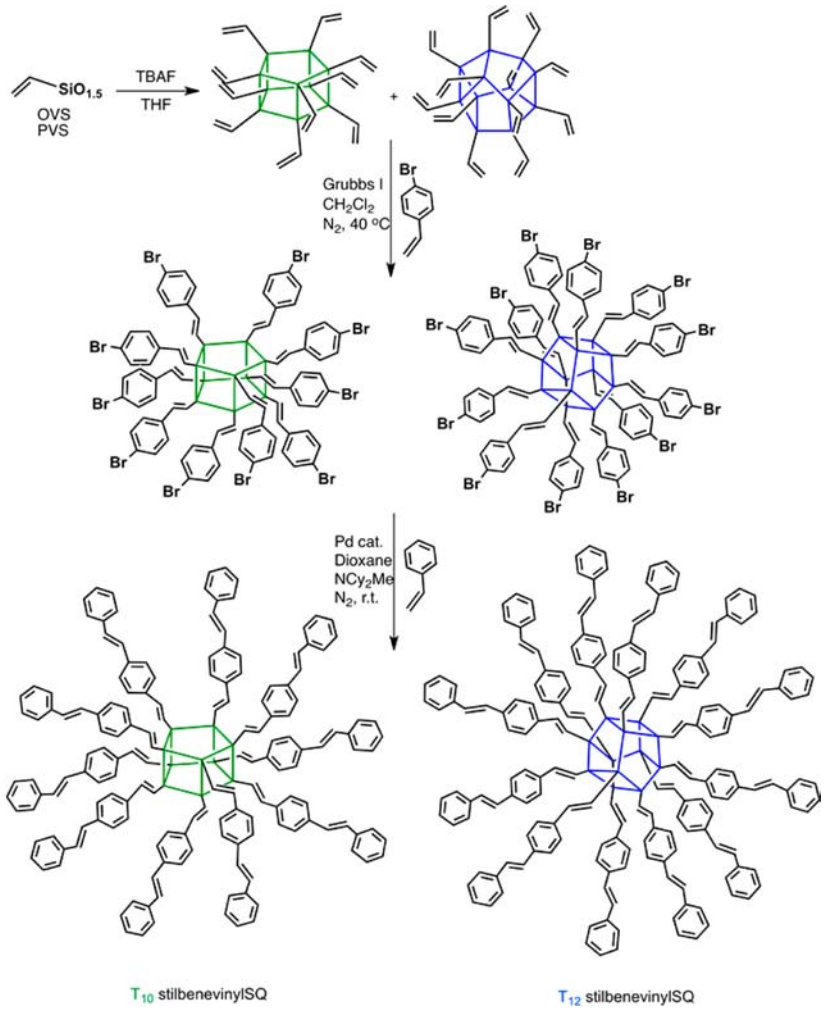

^{1}H NMR (500 MHz, $CDCl_3$) δ 6.3−6.4 (m, $-CH{=}CH_2$), 7.0−7.1 (m, $-CH{=}CH_2$), 7.2−7.3 (m, Ar-*H*), 7.3−7.6 (m, Ar-*H*) ppm; ^{13}C NMR (500 MHz, $CDCl_3$) δ 100.05, 115.00, 126.11, 126.53, 126.69, 127.29, 128.10, 128.66, 135.50, 136.63, 137.14, 138.01 ppm; ^{29}Si NMR (99.35 MHz, $CDCl_3$) δ −78.85 ppm. T_{12} stilbenevinyl-SQ: 3196 amu $[AgSi_{12}O_{18}(C_{16}H_{13})_{12}]$; GPC (found) M_n = 3758, M_w = 3871; PDI = 1.03; ^{1}H NMR (500 MHz, $CDCl_3$) δ 6.3−6.4 (m, $-CH{=}CH_2$), 7.0−7.1 (m, $-CH{=}CH_2$), 7.2−7.3 (m, Ar-*H*), 7.3−7.6 (m, Ar-*H*) ppm; ^{13}C NMR (500 MHz, $CDCl_3$) δ 125.20, 126.54, 126.67, 127.27, 127.36, 127.70, 128.09, 128.67, 129.02, 136.68, 137.10, 137.76, 137.84 ppm; ^{29}Si NMR (99.35 MHz, $CDCl_3$) δ −78.69, −80.44 ppm.

RESULTS AND DISCUSSION

In the following sections, we begin by discussing the synthesis of $T_{10/12}$ stilbenevinyl-SQs via metathesis and Heck cross-coupling reactions. F^--catalyzed rearrangement generates an approximately 1:1 equilibrium mixture of T_{10} and T_{12}.[9,33] We then discuss separating T_{10} and T_{12} stilbenevinyl-SQs by GPC and/or selective precipitation. Thereafter, we detail the solution-based photophysical properties of the pure SQs as compared to *p*-triethoxysilylvinylstilbene, *p*-vinylstilbene, and the T_8 analog.[17] These studies include determining steady-state absorptions and emissions, TPA, and fluorescence lifetime kinetics. Solid-state photophysical properties will be the subject of a future paper, where we will report on novel aggregation.[58]

Synthesis and Separations. Scheme 1 illustrates the general synthesis of the $T_{10/12}$ stilbenevinyl-SQ mixtures; see the Experimental Section for details.

Separation of SQs with different cage sizes is in general an unexplored area given previous difficulties in synthesizing the larger cages, especially the T_{10} SQs. Thus, to date only a few research groups have explored the larger SQ cages.[5,9,14,30,33,34,38,59] As noted above, our motivation for the current studies comes from unexpected differences observed in the photophysical properties of the stilbenevinyl $T_{10/12}$ compared to the T_8 analogs.

To this end, our separation efforts extend the original work of Kawakami et al.[34] Our first attempts assessed direct separation of the vinyl-$T_{10/12}$ mixed starting materials; however, such separations proved difficult due to their high solubility in most solvents combined with oil formation on precipitation into water. We also attempted to separate the individual cages at the 4-bromostyrenyl $T_{10/12}$ stage. While partially successful, separation was not easily reproduced and offered <90% purities. Thus, successful, reproducible separations at purities >95% (MALDI-ToF) came only at the stilbenevinyl-SQ stage.

Our separation method (see the Experimental Section) takes advantage of solubility differences likely due to symmetry differences. Both the T_{10} stilbenevinyl-SQs and the phenyl-SQs,[60] are more soluble than the T_8 and T_{12} compounds and can be separated selectively in high purity but only at 5 mg

dx.doi.org/10.1021/ja4043092 | J. Am. Chem. Soc. 2013, 135, 12259−12269

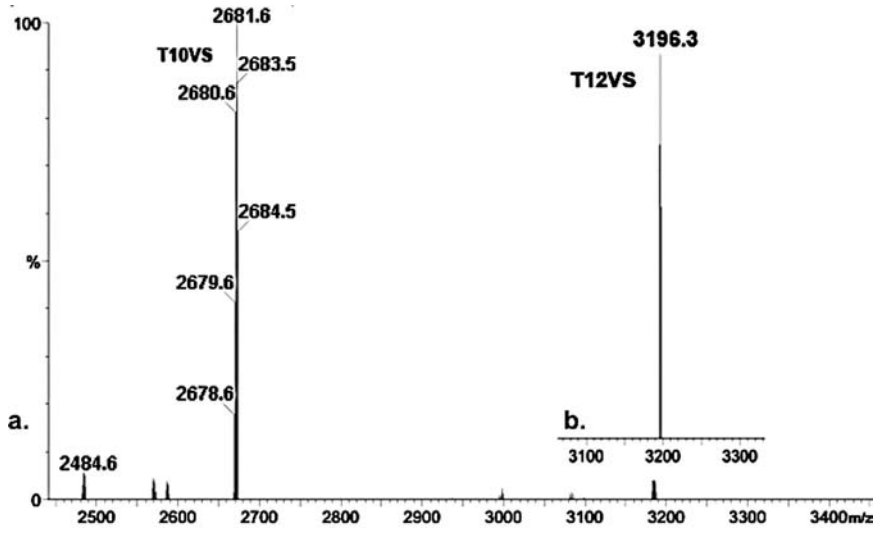

Figure 3. Comparison of the separated (a) T_{10} and (b) T_{12} stilbenevinyl-SQ compounds.

scales (~5% purified recovery). This follows efforts to separate these compounds via silica gel column chromatography, affinity chromatography using dodecaphenyl-SQ as the column media, gel permeation chromatography (GPC), and selective solubility. Only GPC and selective solubility approaches work well with the latter, providing better separation of T_{10}, due to its higher solubility. Thus, GPC was better for purifying T_{12} after T_{10} removal. Up to eight iterations were necessary to purify T_{12} without GPC. Only two iterations were necessary to purify T_{10}. Figure S1 (Supporting Information) provides a schematic of the solubility-based separations.

The separated materials were characterized as described below and in the Experimental Section. The most notable verifications of purity are MALDI-TOF mass spectral analysis and ^{29}Si NMR. Parts a and b of Figure 3 compare the T_{10} and T_{12} stilbenevinyl-SQs MALDI-TOF spectra, showing successful separation. Table 1 shows the ^{29}Si NMR ppm shift for selected species, with the spectra shown in Figure S2 and S3 (Supporting Information) offering corroborative proof of the separation efficiency.

Table 1. ^{29}Si NMR Chemical Shift Values for the Separated Stilbenevinyl-SQ Cages

compd	chemical shift (ppm)
T_8 stilbenevinyl-SQ	−78.17
T_{10} stilbenevinyl-SQ	−78.85
T_{12} stilbenevinyl-SQ	−78.69, −80.44

Photophysical Characterization. *Steady-State Spectroscopy.* Successful separation allowed us to map the photophysical properties. The first step was to compare the absorption (Figure 4a) and emission spectra (Figure 4b) of the individual T_{10} and T_{12} compounds.[9] The absorption spectra show similar band structures and maxima for all the cage species ($T_{8,10,12}$) with absorption peaks at 320, 333, and 352 nm. Figure 4b shows the emission spectra of the stilbenevinyl-SQs normalized to the same absorption value (λ_{max} = 0.6).

Surprisingly, stilbenevinyl-T_{12} gives the lowest emission intensities with Φ_{PL} = 11%, despite having the greatest number of chromophores. This suggests that there is more nonradiative decay through self-absorption with the greater number of chromophores.[61] Indeed, this would be expected if we also recall that the "bite" angle for this molecule averages 60° (vs 72° for T_{10} and 90° for T_8), placing the functional groups in closer proximity to each other and improving the opportunity for self-absorption.[21] The *p*-triethoxylsilylvinylstilbene shows the highest quantum yield at 38%. The absorption and emission spectra for this compound are given in Figure S4 (Supporting Information). Table 2 shows the molar extinction coefficients, absorption and emission maxima, and quantum yields.

Photophysical characterization at different excitation wavelengths suggests the existence of two emissive states in stilbenevinyl-SQs at low concentrations (<1 μM in THF). Figure 5a compares the excitation spectra for the T_{10} and T_{12} stilbenevinyl-SQs for two different emission wavelengths, which is of importance in our two-photon absorption study below (450, 387 nm). Both give similar excitation spectra, with only the 450 nm excitation spectrum showing a slight shoulder between 380 and 420 nm. This is initial evidence of the existence of multiple emissive states in these molecules.

The shoulder seen in the excitation spectrum may give rise to the red-shifted emissive state in the 436−450 nm range, since Figure 5b shows that the relative intensities of the fluorescence spectra correlate well with the amplitude of the shoulder. This figure compares the emission spectra from different excitation bands (333 and 400 nm). Note that a red shift is observed on shifting the excitation wavelength to higher values. Excitation at <375 nm provides emission λ_{max} = 385 nm. In contrast, excitation at >375 nm red shifts the emission to $\lambda_{max} \approx$ 450 nm. This excitation based spectral shift is found in all cages per Figures S5 and S6 (Supporting Information) and is slightly observable in the *p*-triethoxylsilylvinylstilbene (<1%, Figure S7, Supporting Information); however, it is not seen in the *p*-vinylstilbene (Figure S8, Supporting Information). These spectral shifts are unusual for organic systems, but since we are dealing with rigid 3-D hybrid materials, with chromophores oriented in space, various excited state energy transfer processes are possible, allowing access to red-shifted emissive states.

This red shift can potentially be attributed to a "red-edge" effect, typically observed for locked fluorophores with well-defined dipole moments in highly viscous solvents; however, it has also been observed for fluorophores attached to rigid substrates and often results from lower rotational diffu-

dx.doi.org/10.1021/ja4043092 | J. Am. Chem. Soc. 2013, 135, 12259−12269

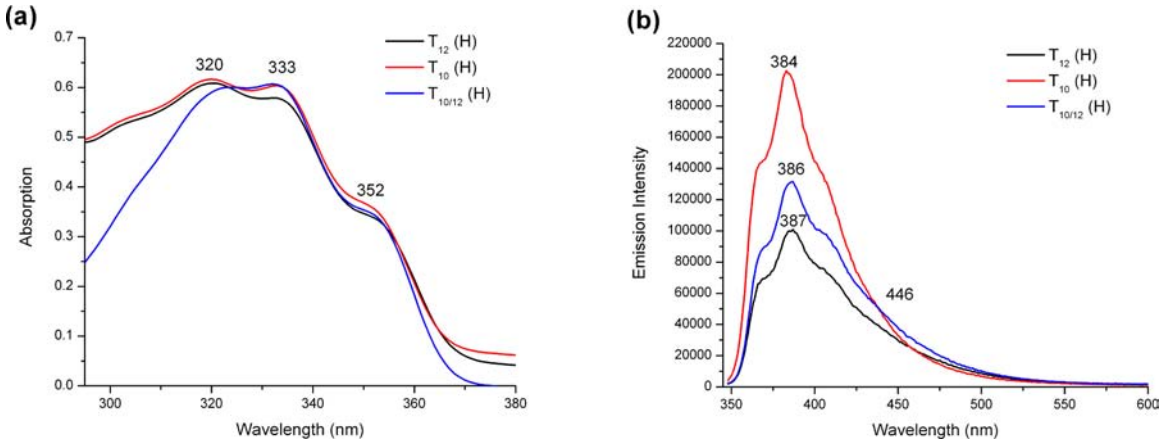

Figure 4. (a) Absorption spectra and (b) emission spectra (THF, ~3 × 10^{-7} M) of stilbenevinyl-SQs.

Table 2. Comparison of Steady-State Properties in THF

	λ_{max} (nm)			
	Abs	Em	ε (M^{-1} cm^{-1})	Φ_{PL} %
T_8 (H)	335	385	286 000	36
T_{10} (H)	333	383	358 000	19
T_{12} (H)	333	386	430 000	11
$T_{10/12}$ (H)	333	387	394 000	15
p-triethoxysilyl-VS	329	380	38 200	38
p-vinylstilbene	328	373	35 800	28

sion.[61−63] Since SQs are very rigid substrates that would force fluorophores into certain conformations on the basis of a structure that may be thought of as a nearly solvent-free environment and that also show dipolar effects (see TPA), what is observed appears to be a novel example of the red-edge effect.

The 450 nm emission is close to the emission maximum found in solid-state analyses, which will be explored further in a subsequent paper on solid state and aggregation effects on these materials (Figures S9 and S10, Supporting Information),[58] but due to the low concentrations used, it is unlikely that molecules are in close enough proximity to interact as if they were in the solid state (i.e., aggregates). However theoretical calculations and kinetic studies suggest that chromophore−chromophore interactions may still be possible.[64,65] Another explanation could be that the organic group emissions in the solid state and in any aggregates that form are quenched, so that the 450 nm emission dominates the 387 nm band. The low-energy tailing present in the 387 nm emission suggests that the 450 nm emission is present regardless of excitation wavelength but is masked by the higher Φ_{PL} of the 387 nm emission.

Two-Photon Absorption. Two-photon spectroscopy was used to compare the polarization and nonlinear absorption properties of the separated cages, *p*-triethoxylsilylvinylstilbene, and *p*-vinylstilbene. Tables 3 and 4 compare the two-photon cross sections at three laser excitation wavelengths (650, 740, and 800 nm). The 800 nm excitation shows the greatest

Table 3. Comparison of TPA data for (H)-Stilbenevinyl-SQs (cross sections GM/mol)

sample	concn (M)	800 nm δ (GM)	740 nm δ (GM)	650 nm δ (GM)
$T_{10/12}$ (H)	1.94 × 10^{-6}	30	52	41
T_{12} (H)	1.42 × 10^{-6}	7	40	63
T_{10} (H)	1.57 × 10^{-6}	42	55	57
T_8 (H)	2.35 × 10^{-6}	2.0	16	26
p-triethoxysilyl-VS	1.03 × 10^{-5}	0.2	1.1	N/A
p-vinylstilbene	1.04 × 10^{-5}	N/A	0.5	2

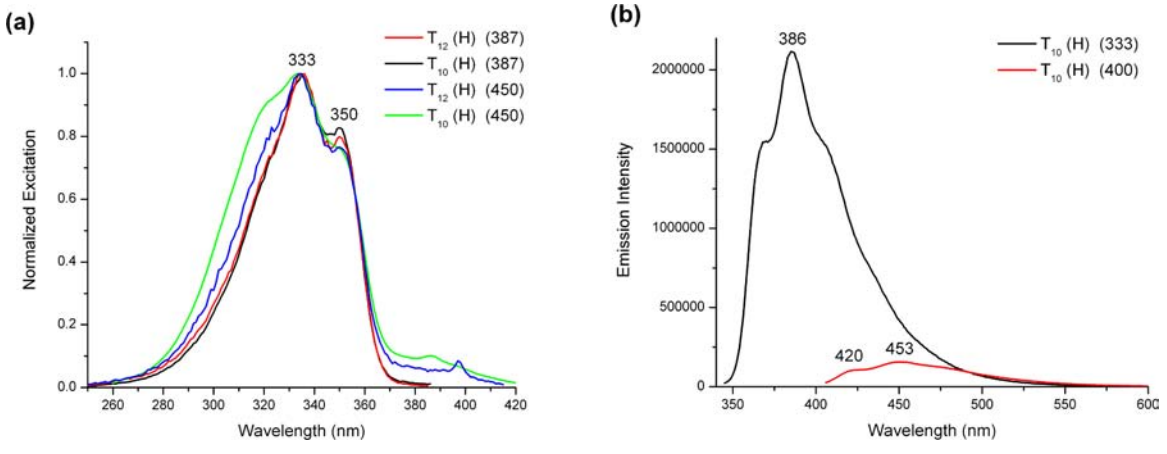

Figure 5. (a) Comparison of excitation spectra for T_{10} and T_{12} stilbenevinyl-SQ with emission held at 387 and 450 nm. (b) Comparison of emission of T_{10} stilbenevinyl-SQ with excitation at 333 or 400 nm (THF, ~2 × 10^{-7} M).

dx.doi.org/10.1021/ja4043092 | J. Am. Chem. Soc. 2013, 135, 12259−12269

Table 4. TPA Data for (H)-Stilbenevinyl-SQs (cross sections GM/chromophore)

sample	800 nm/chrom δ (GM)	740 nm/chrom δ (GM)	650 nm/chrom δ (GM)
$T_{10/12}$ (H)	2.7	4.7	3.8
T_{12} (H)	0.6	3.3	5.3
T_{10} (H)	4.2	5.5	5.7
T_8 (H)	0.3	2.0	3.3

differences between cross sections, with T_{10} giving the largest cross section at ~42 GM/mol. This suggests that the T_{10} cage has the largest change in dipole moment on excitation.[57,66,67] Due to their different symmetries, the two structural formats will have different two-photon selection rules based on orbital geometry and thus different polarization dynamics, likely accounting for the different TPA cross section values.[68,69]

This then represents a relatively novel observation given that few 3-D molecular species are available with identical moieties and overall compositions that also offer quite different geometries. Thus, our results are the first examples for such classes of compounds.

Figure 6 shows the two-photon excited fluorescence (TPEF) spectra at 800 nm, with T_{10} showing the highest fluorescence intensity at equal concentrations. The interesting observation is that with 740 and 800 nm excitation, the emission wavelength is ~450 nm, which is similar to the one-photon emission band from excitation at 370 and 400 nm (Table 5). Figure S11 (Supporting Information) shows the log–log plot for cross section calculations at 740 nm, with a slope of 2 guaranteeing a quadratic dependence on excitation energy.

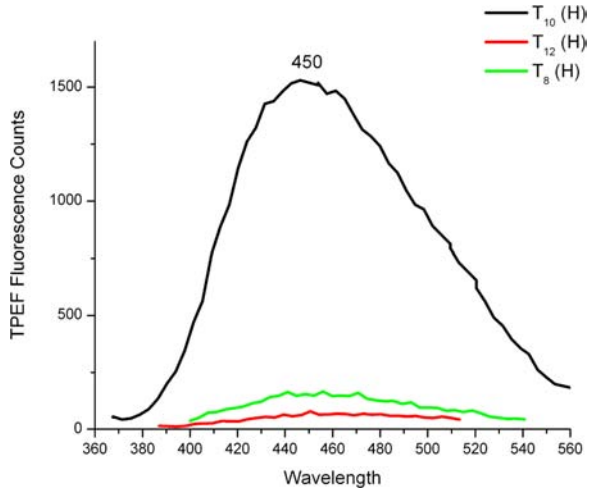

Figure 6. TPEF plot comparing $T_{8,10,12}$ stilbenevinyl-SQs at 800 nm excitation.

Table 5. TPEF Emission Maxima at Different Two-Photon Excitation Wavelengths

sample	800 nm	740 nm	650 nm
$T_{10/12}$ (H)	455	466	410
T_{12} (H)	453	473	411
T_{10} (H)	458	461	415
T_8 (H)	452	464	407
p-triethoxysilyl-VS	439	432	
p-vinylstilbene		395	395

Two-photon spectroscopy at 650 nm shows emission maxima between 407 and 415 nm for the single cage SQs, most consistent with one-photon emission from excitation at 335 nm, with only a 20 nm red shift as opposed to 60 nm for the other excitations (Tables 3 and 4). The TPA cross sections are comparable to those found at 740 nm excitation. The *p*-triethoxysilylvinylstilbene gives a cross section at 800 and 740 nm of 0.2 and 1.1 GM respectively; however, data at 650 nm is unavailable at this time. Also note that the cross sections of this compound are smaller than the per chromophore values for the cages.

A further important observation is that *p*-vinylstilbene itself does not show a TPA excitation or cross section at 800 nm and only a small cross section at 740 nm of 0.5 GM. A cross section of 2 GM is reasonable for excitation at 650 nm; however, it is still nearly half that of the per chromophore values for the cage compounds. *Therefore, depending on the wavelength (i.e., 740 nm), the cages offer at least a 10-fold TPA enhancement over their organic counterparts and at least 2-fold over their hybrid model.* TPA enhancements of the SQs at 650 nm are only double that of organic alone.

This TPA observation suggests that the SQs offer greater electronic coupling, especially at longer wavelengths, which is important for efficient energy transfer processes, such as electron/hole pair separation. This polarization is 3D in nature and thus is likely highly symmetry dependent. A larger two-photon cross section also scales with a higher absorption efficiency at low excitation intensity, which is related to the large density of chromophores surrounding the core, which is contained in a small unit volume with spherical diameter of ~1.5 nm. This allows for molecules to more efficiently absorb light over a broad range of light intensity and give enhanced cross sections.

Since these molecules have two emission states dependent on the excitation wavelength, it is necessary to take into account the quantum yield differences between the emission bands for an accurate TPA cross section calculation. Table 6 shows the quantum yields (QYs) for the two emission bands, in which the red-shifted emission band (450 nm) is ≈10% of the 386 nm emission band.

Fluorescence Lifetime Kinetics. Fluorescence upconversion measurement analyses were carried out in THF. Analyses were done at excitation wavelengths of 286 and 400 nm and then collected at 385 and/or 450 nm to measure the fluorescence kinetics for each of the two states described

Table 6. Quantum Yield Values for the Two Emission Bands

sample	QY_{387nm}	QY_{450nm}
$T_{10/12}$ (H)	0.15	0.012
T_{12} (H)	0.11	0.011
T_{10} (H)	0.19	0.018
T_8 (H)	0.36	0.039
p-triethoxysilyl-VS	0.38	
p-vinylstilbene	0.24	

dx.doi.org/10.1021/ja4043092 | J. Am. Chem. Soc. 2013, 135, 12259–12269

Table 7. Fluorescence Lifetime Data for 286 nm Excitation and 450 nm Collection (Isotropy)

	T_1 (fs)	A_1	T_2 (ps)	A_2	T_3 (ps)	A_3
T_8	760	−0.36	16 ± 2	0.33	209 ± 47	0.46
T_{10}	840	−0.29	15 ± 4	0.39	167 ± 47	0.54
T_{12}	950	−0.29	11 ± 4	0.18	155 ± 20	0.62
$T_{10/12}$	900	−0.21	17 ± 6	0.14	170 ± 35	0.55
p-triethoxysilyl-VS	0	0	6.1 ± 0.9	0.16	252 ± 6	0.98
p-vinylstilbene	0	0	2.9 ± 0.5	0.37	49 ± 5	0.38

above and to investigate the potential for charge transfer.[70−72] The long component lifetimes were run for hundreds of picoseconds for each compound.

Table 7 and Figures 7 and 8 compare lifetimes for the stilbenevinyl-SQs as compared to *p*-triethoxylsilylvinylstilbene

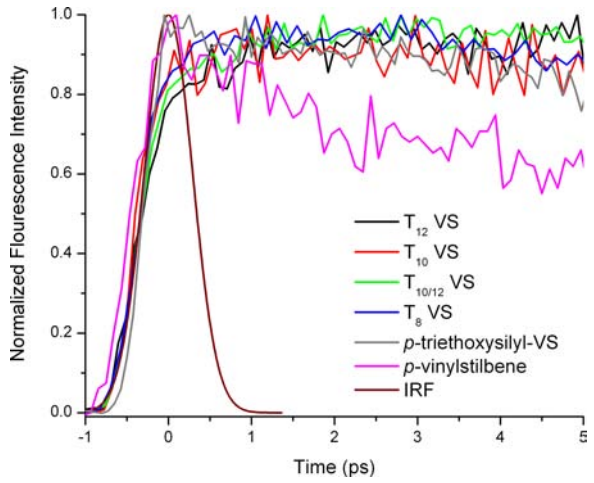

Figure 7. Comparsion of short fluorescence liftetime components of stilbenevinyl-SQs with the instrument response function at 286 nm.

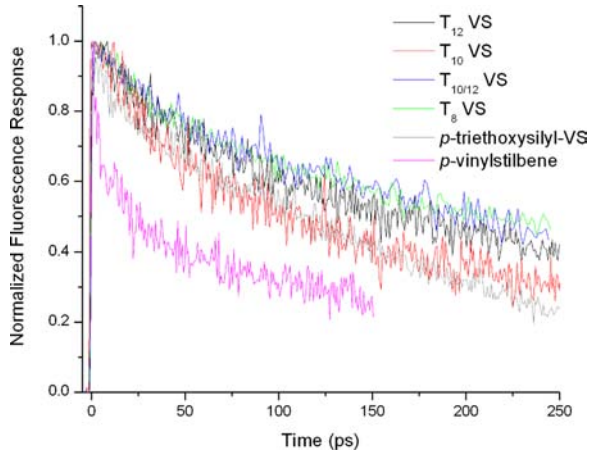

Figure 8. Comparison of long decay fluorescence lifetime components of stilbenevinyl-SQs.

and *p*-vinylstilbene with an excitation at 286 nm and an emission collection at 450 nm. These studies were done to probe the red-shifted fluorescence band shown above and show that, within error, all the cages give similar lifetimes for their short (T_2) and long (T_3) components. Note that in Figure 7, the T_{10} stilbenevinyl-SQ shows a stronger T_2 component, which results in its long decay being below, but parallel to, those of the other stilbenevinyl-SQs. This can be attributed to the symmetry differences in the T_{10} system, which likely also contribute to its enhanced TPA cross section over the other cage sizes. The *p*-triethoxylsilylvinylstilbene gives a lifetime that is just slightly longer than those for the SQ cages (~252 ps), which can be attributed to the higher QY.

The outlier in this study was *p*-vinylstilbene (free chromophore), which shows much shorter lifetimes of 2.9 and 49 ps, respectively. This is expected since the degree of rotational diffusion should be largest in the free chromophore.[61] This may also suggest a shorter-lived excited state than the hybrid systems, likely due to the influence of silicon.

The "rise time" (T_1) was determined for these compounds, which is the onset time for fluorescence to occur from the probed state and often indicative of an excited state process.[61,70,72−74] Excitation at 286 nm and emission collection at 450 nm gave a rise time of a few hundred femtoseconds, suggesting that the 450 nm emission comes from a lower energy excited state.

This suggests that it takes time after the molecule is excited to fluoresce from that state, giving evidence for an energy transfer process.[61] Figures S12−S15 (Supporting Information) compare the stilbenevinyl-SQs with and without rise time fits. Two compounds shown in Table 7 and Figure 7 that did not show a rise time were the free chromophore systems (*p*-triethoxylsilylvinylstilbene and *p*-vinylstilbene). Our analysis shows that the shortest rise times are observed for the T_8 stilbenevinyl system at 760 fs, while the T_{10} gives a rise time of 840 fs and the T_{12} a rise time of 950 fs, suggestive of Förster energy transfer.[75−77]

There are two primary charge transfer mechanisms that may be expected in these molecules, but they may or may not be related to these rise times, as other solvent and symmetry effects are plausible.[78] The first is a Dexter energy transfer from the stilbenevinyl groups to the cage. The second is Förster-type hopping between chromophores, which could occur on the same cage or between cages. Our rise times discussed above are on the time scale where Förster energy transfer (FRET) takes place, which would suggest it as an energy transfer mechanism for these systems.[75−77] This however does not rule out the possibility of a Dexter-type energy transfer from chromophore to cage, as this transfer would be faster than the instrument response function (650 fs) and could not be observed by our methods. Therefore, it is possible that both mechanisms proceed, but further analysis and computational modeling is necessary.

In order to gain a better understanding of the FRET system, we calculated the Förster radii for the compounds.[61,75] For the calculation, we used the assumption that the dipolar angles would scale with the angles between the chromophores discussed above and the integral of the overlap between absorption and emission spectra. We calculate the Förster radius R_0 to be ~12 Å for T_8, 10 Å for T_{10}, and 8.6 Å for T_{12}. If we then approximate the distance between chromophores from

dx.doi.org/10.1021/ja4043092 | J. Am. Chem. Soc. 2013, 135, 12259−12269

a combination of similar crystal structures and computational modeling, we get values for the centroid−centroid distance of two adjacent chromophores to be ∼12, 14, and 16 Å, respectively.[5] Back-calculation of the expected lifetimes are on the order of a few hundred femtoseconds to a few picoseconds, depending on the exact distance (r) chosen between chromophores. From our analysis, the best energy transfer would likely occur within the first few carbons on the cage side of the chromophores (∼7−9 Å between chromophores), which are within the Förster radii discussed above and may involve the face of the cage. Förster energy transfer between the outside (ends) of the chromophores (>20 Å) is unlikely for these systems.

Early theoretical modeling attempts suggest that Förster hopping between chromophores on the same cage is most likely at 10^{-7} M concentrations,[64,65] which would also be expected for the solid state, and is observed in its emission data. Their calculations show that charge transfer by this method is solvent stabilized. However, unpublished experimental analyses of single chromophore (mono-stilbenevinyl-SQ) systems suggests that, if this is true, it is not necessarily between chromophores on the same cage, since similar steady-state spectra are observed for the fully functionalized systems.[58] In order to fully understand the mechanisms by which this rise time occurs, we are assessing the photophysical properties of single chromophore SQs, allowing for simplification of the energy transfer possibilities.[58]

Table 8 shows the fluorescence lifetimes of $T_{10/12}$ stilbenevinyl-SQ taken previously. This compound was excited

Table 8. Fluorescence Lifetimes of Selected Stilbenevinyl-SQ Components Excited at 286 nm with Fluorescence Collection at 385 nm

	T_1 (ps)	A_1	T_2 (ps)	A_2
$T_{10/12}$	20 ± 5	0.27	140 ± 82	0.39

at 286 nm and probed at 385 nm, the main fluorescence band. The $T_{10/12}$ compound shows lifetimes of 20 and 140 ps, respectively, which is within error for that found in the study above. No rise time was observed for this excitation-probe pair, suggesting that this fluorescence is directly from the chromophore emission.

Table S1 and Figure S16 (Supporting Information) show the fluorescence lifetimes of the stilbenevinyl-SQs with excitation at 400 nm and emission probing at 450 nm. As this was our first kinetic analysis of stilbenevinyl-SQ-based materials, a more careful analysis is needed for the 400 nm excitation data, since this is an off-band wavelength, and it will be discussed in further detail in a subsequent publication.[58]

Polarized excitation measurements for these materials give fluorescence anisotropy for the stilbenevinyl-SQs. The anisotropy shows the directionality of the materials, such that a more symmetrical and less freely moving material gives a higher anisotropy value (max of 0.4).[79,80] The anisotropy was measured for the 286 nm excitation and 450 nm collection. The T_8 compound shows higher anisotropy (0.3/0.4) than the T_{10} (0.1) or T_{12} (0.15). This means that the highest symmetry and lowest directional dependence is observed for the T_8 system (Figure 9). The *p*-triethoxylsilylvinylstilbene also shows medium anisotropy that decays from 0.2 to nearly 0 in 250 ps.

The $T_{10/12}$ stilbenevinyl-SQ mixture also shows low anisotropy similar to that of the T_{10}. The anisotropy does

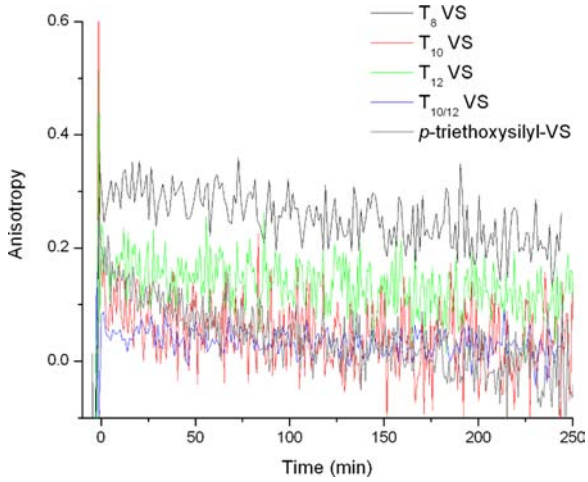

Figure 9. Fluorescence anisotropy measured at 286 nm excitation and 450 nm fluorescence collection for stilbenevinyl-SQs.

not decay significantly during the 250 ps measurement time. The decrease in anisotropy for regular organic systems can be attributed to two factors, increased rotational diffusion and/or increased energy transfer processes.[61] The likelihood of radiationless energy transfer likely increases in the larger cage systems due to the closer proximity of the chromophores even under micromolar concentrations.[81−83]

The only extensively studied 3-D systems are those of fullerenes, which offer excellent charge delocalization and show even lower anisotropy values of ∼0.5.[50] Therefore, we can speculate that the larger SQs also show charge delocalization in 3-D based on a combination of known properties of organic systems and observations from fullerenes.

SUMMARY OF FINDINGS

In the above studies we found the following:

(1) It was possible to purify T_{10} and T_{12} stilbenevinyl-SQs by selective solubility/precipitation methods by exploiting the geometric differences between the cages.

(2) Higher chromophore densities per cage decrease fluorescence quantum yields, contrary to expectations but likely due to enhanced self-absorption leading to nonradiative decay processes.

(3) Single-photon and two-photon excitation dependent emissions that can be attributed to red-edge effects.

(4) Of the three cage sizes and symmetries studied, the T_{10} stilbenevinyl-SQs offer the highest TPA cross sections, indicative of the strongest electronic coupling and polarization.

(5) SQ cage compounds show "rise times" of 700−1000 fs and low anisotropies (∼0.1) in fluorescence upconversion lifetime kinetic studies, indicative of an excited-state energy transfer process (internal delocalization or FRET-type energy transfer), which is unobserved for the free chromophore, unexpected for a system with an "inert" silica core, and unexpected for 3-D hybrid molecular species.

CONCLUSIONS

The separated T_{10} and T_{12} stilbenevinyl-SQs show properties that are unique to their cage sizes and symmetries. First, we see decreases in fluorescence quantum yield with increasing cage sizes, indicative of self-quenching effects likely due to cage symmetry and/or chromophores' proximity. Second, stilbenevinyl-SQs show excitation-dependent emission in both one-

dx.doi.org/10.1021/ja4043092 | J. Am. Chem. Soc. 2013, 135, 12259−12269

photon and two-photon absorption studies, evidence of a red-edge effect, an unusual result normally observed for fluorophores attached to 2-D rigid substrates.

The current studies identify the existence of red-edge effects in 3-D molecular structures and suggest a new class of hybrid materials offering switchable emissions. In addition, the T_{10} stilbenevinyl-SQ exhibits the highest enhanced TPA cross section, implying the highest polarizability (charge separation), which can be attributed directly to its symmetry. This is again a first example of the effects of symmetry in a class of 3-D molecules that are essentially identical in all other aspects. Lastly, fluorescence lifetime kinetics and anisotropy measurements show that stilbenevinyl-SQs offer charge delocalization in the excited state through a likely combination of Förster and Dexter energy transfer processes, while the free chromophores do not. The process by which this transfer occurs will be under further investigation but can be described as through cage (cage−chromophore), through space (chromophore−chromophore), or by both processes simultaneously.

The observation of 3D charge delocalization, high absorption efficiencies, and high cross sections shows that we can potentially tailor SQs for use in electronic and photonic applications. This is the first study mapping the detailed photophysical properties of T_{10} and T_{12} silsesquioxanes and the first evidence of quite different photophysical properties based solely on cage size and symmetry.

■ ASSOCIATED CONTENT

Supporting Information

Further characterization information of synthesized compounds and further spectroscopic data. This material is available free of charge via the Internet at http://pubs.acs.org.

■ AUTHOR INFORMATION

Corresponding Author

talsdad@umich.edu; tgoodson@umich.edu

Notes

The authors declare no competing financial interest.

■ ACKNOWLEDGMENTS

The synthesis, separations and spectroscopic work was supported by the U.S. Department of Energy (DOE), Office of Basic Energy Sciences, as part of the University of Michigan Center for Solar and Thermal Energy Conversion Energy Frontier Research Center, No. DE-SC0000957. NMR characterization studies were supported by Intel Corp. through contract number MSR-Intel Task 2170.001. We would also like to thank Dr. Oleg Varnavski for all his help with the upconversion measurements. R.M.L. would like to thank the Technion Dept of Mechanical Engineering, Haifa, Israel, for a Lady Davis Fellowship, where portions of this manuscript were written.

■ REFERENCES

(1) Hartmann-Thompson, C. In *Applications of Polyhedral Oligomeric Silsesquioxanes SE-7*; Hartmann-Thompson, C., Ed.; Springer: Netherlands, 2011; Vol. 3; pp 247−325.

(2) Kaneko, Y.; Coughlin, E. B.; Gunji, T.; Itoh, M.; Matsukawa, K.; Naka, K. *Int. J. Polym. Sci.* **2012**, *2012*, 1−2.

(3) Chan, K. L.; Sonar, P.; Sellinger, A. *J. Mater. Chem.* **2009**, *19*, 9103.

(4) Laine, R. M.; Sulaiman, S.; Brick, C.; Roll, M.; Tamaki, R.; Asuncion, M. Z.; Neurock, M.; Filhol, J.-S.; Lee, C.-Y.; Zhang, J.; Goodson, T.; Ronchi, M.; Pizzotti, M.; Rand, S. C.; Li, Y. *J. Am. Chem. Soc.* **2010**, *132*, 3708−3722.

(5) Roll, M. F.; Kampf, J. W.; Kim, Y.; Yi, E.; Laine, R. M. *J. Am. Chem. Soc.* **2010**, *132*, 10171−10183.

(6) Choi, J.; Yee, A. F.; Laine, R. M. *Macromolecules* **2003**, *36*, 5666−5682.

(7) Samthong, C.; Laine, R. M.; Somwangthanaroj, A. *J. App. Polym. Sci.* **2013**, *128*, 3601−3608.

(8) Lin, W.; Chen, W.; Wu, W.; Niu, Y.; Jen, A. *Macromolecules* **2004**, *37*, 2335−2341.

(9) Jung, J. H.; Furgal, J.; Goodson, T., III; Mizumo, T.; Schwartz, M.; Chou, K.; Vonet, J.-F.; Laine, R. M. *Chem. Mater.* **2012**, *24*, 1883−1895.

(10) Neumann, D.; Fisher, M.; Tran, L.; Matisons, J. G. *J. Am. Chem. Soc.* **2002**, *124*, 13998−13999.

(11) Hong, B.; Thoms, T. P. S.; Murfee, H. J.; Lebrun, M. J. *Inorg. Chem.* **1997**, *36*, 6146−6147.

(12) Laine, R. M.; Roll, M. F. *Macromolecules* **2011**, *44*, 1073−1109.

(13) Kim, Y.; Koh, K.; Roll, M. F.; Laine, R. M.; Matzger, A. J. *Macromolecules* **2010**, *43*, 6995−7000.

(14) Baney, R. H.; Itoh, M.; Sakakibara, A.; Suzuki, T. *Chem. Rev.* **1995**, *95*, 1409−1430.

(15) Sulaiman, S.; Zhang, J.; Goodson, T., III; Laine, R. M. *J. Mater. Chem.* **2011**, *21*, 11177.

(16) Laine, R. M.; Soles, C. L.; Krug, D. J.; Wook Ro, H.; Popova, V. Silsesquioxane Derived Hard, Hydrophobic, and Thermally Stable Thin Films and Coatings for Tailorable Protective and Multi-Structured Surfaces and Interfaces. U.S. Patent Appl. 20110062619 A1, March 17, 2011.

(17) Sulaiman, S.; Bhaskar, A.; Zhang, J. *Chem. Mater.* **2008**, *20*, 5563−5573.

(18) Lo, M. Y.; Zhen, C.; Lauters, M.; Jabbour, G. E.; Sellinger, A. *J. Am. Chem. Soc.* **2007**, *129*, 5808−5809.

(19) Voronkov, M.; Lavrent'yev, V. *Top. Curr. Chem.* **1982**, *102*, 199−236.

(20) Loy, D.; Shea, K. *Chem. Rev.* **1995**, *95*, 1431−1442.

(21) Calzaferri, G. *Tailor-Made Silicon−Oxygen Compounds, from Molecules to Materials*; Corriu, R., Jutzi, P., Eds.; Springer: New York, 1996; p 149.

(22) Lichtenhan, J. In *Polymeric Materials Encyclopedia*; Salmone, J. C., Ed.; CRC Press: New York, 1996; pp 7768−7777.

(23) Provatas, A.; Matisons, J. G. *Trends. Polym. Sci.* **1997**, *5*, 327−333.

(24) Li, G.; Wang, L.; Ni, H.; Pittman, C. U., Jr. *J. Inorg. Organomet. Polym.* **2002**, *11*, 123−154.

(25) Duchateau, R. *Chem. Rev.* **2002**, *102*, 3525−42.

(26) Phillips, S. H.; Haddad, T. S.; Tomczak, S. J. *Curr. Opin. Solid State Mater. Sci.* **2004**, *8*, 21−29.

(27) Abe, Y.; Gunji, T. *Prog. Polym. Sci.* **2004**, *29*, 149−182.

(28) Kannan, R. Y.; Salacinski, H. J.; Butler, P. E.; Seifalian, A. M. *Acc. Chem. Res.* **2005**, *38*, 879−84.

(29) Laine, R. M. *J. Mater. Chem.* **2005**, *15*, 3725.

(30) Lickiss, P. D.; Rataboul, F. *Adv. Organomet. Chem.* **2008**, *57*, 1−116.

(31) Wu, J.; Mather, P. T. *Polym. Rev.* **2009**, *49*, 25−63.

(32) Cordes, D. B.; Lickiss, P. D.; Rataboul, F. *Chem. Rev.* **2010**, *110*, 2081−173.

(33) Asuncion, M. Z.; Laine, R. M. *J. Am. Chem. Soc.* **2010**, *132*, 3723−36.

(34) Miyazato, A.; Pakjamsai, C.; Kawakami, Y. *Dalton Trans.* **2010**, *39*, 3239−44.

(35) Ronchi, M.; Sulaiman, S.; Boston, N. R.; Laine, R. M. *Appl. Organomet. Chem.* **2009**, *24*, 551−557.

(36) Harrison, D. P.; Hall, C. *Main Group Met. Chem.* **1997**, *20*, 515.

(37) Agaskar, P. *Inorg. Chem.* **1991**, 2707−2708.

(38) Brown, J. F. *J. Am. Chem. Soc.* **1965**, *87*, 4317−4324.

(39) Jung, J. H.; Furgal, J. C.; Clark, S. C.; Schwartz, M.; Chou, K.; Laine, R. M. *Macromolecules*, submitted.

(40) Furgal, J. C.; Jung, J. H.; Clark, S. C.; Goodson, T., III; Laine, R. M. *Macromolecules*, submitted.
(41) Varnavski, O.; Yan, X.; Mongin, O.; Blanchard-Desce, M.; Goodson, T. *J. Phys. Chem. C* **2006**, *111*, 149−162.
(42) Goodson, T. G. *Acc. Chem. Res.* **2005**, *38*, 99.
(43) Xu, C.; Webb, W. W. *J. Opt. Soc. Am. B* **1996**, *13*, 481.
(44) Haley, J. E.; Krein, D. M.; Monahan, J. L.; Burke, A. R.; McLean, D. G.; Slagle, J. E.; Fratini, A.; Cooper, T. M. *J. Phys. Chem. A* **2010**, *115*, 265−273.
(45) Jha, P. C.; Das, M.; Ramasesha, S. *J. Phys. Chem. A* **2004**, *108*, 6279−6285.
(46) Varnavski, O.; Goodson, T. G., III *Chem. Phys. Lett.* **2000**, 688−696.
(47) Ramakrishna, G.; Bhaskar, A.; Goodson, T., III *J. Phys. Chem. B* **2006**, *110*, 20872−8.
(48) Flynn, D. C.; Ramakrishna, G.; Yang, H.; Northrop, B. H.; Stang, P. J.; Goodson, T. G., III *J. Phys. Chem. B.* **2010**, 1348−1358.
(49) Raymond, J. E.; Goodson, T. *J. Phys. Chem. Lett.* **2011**, *2*, 329−333.
(50) Fedorov, A.; Berberan-Santos, M. N.; Lefevre, J.-P.; Valeur, B. *Chem. Phys. Lett.* **1997**, *267*, 467−471.
(51) Brusatin, G.; Signorini, R. *J. Mater. Chem.* **2002**, *12*, 1964−1977.
(52) Amendola, V.; Mattei, G.; Cusan, C.; Prato, M.; Meneghetti, M. *Synth. Met.* **2005**, *155*, 283−286.
(53) Liu, Z.; Xu, Y.; Zhang, X.; Zhang, X.; Chen, Y.; Tian, J. *J. Phys. Chem. B.* **2009**, 9681−9686.
(54) Peterson, J. J.; Simon, Y. C.; Coughlin, E. B.; Carter, K. R. *Chem. Commun.* **2009**, 4950−2.
(55) Peterson, J. J.; Werre, M.; Simon, Y. C.; Coughlin, E. B.; Carter, K. R. *Macromolecules* **2009**, *42*, 8594−8598.
(56) Maciejewski, A.; Steer, R. *J. Photochem.* **1986**, *35*, 59−69.
(57) Bhaskar, A.; Ramakrishna, G.; Lu, Z.; Twieg, R.; Hales, J. M.; Hagan, D. J.; Van Stryland, E.; Goodson, T., III *J. Am. Chem. Soc.* **2006**, *128*, 11840−9.
(58) Furgal, J. C.; Abeyasinge, N.; Yi, E.; Goodson, T.; Laine, R. M. Manuscript in preparation.
(59) Rikowski, E.; Marsmann, H. C. *Polyhedron* **1997**, *16*, 3357−3361.
(60) Bahrami, M.; Furgal, J. C; Hashemi, H.; Cao, F.; Kieffer, J.; Laine, R. M. Manuscript In preparation.
(61) Lakowicz, J. *Principles of Fluorescence Spectroscopy*; 3rd ed.; Springer Science+Business Media: New York, 2006; pp 47, 243, 358−359, 588.
(62) Demchenko, A. P. *Luminescence* **2002**, *17*, 19−42.
(63) Józefowicz, M.; Heldt, J. R. *J. Fluoresc.* **2011**, *21*, 239−45.
(64) Phillips, H.; Zheng, S.; Hyla, A.; Laine, R.; Goodson, T.; Geva, E.; Dunietz, B. D. *J. Phys. Chem. A* **2012**, *116*, 1137−1145.
(65) Zheng, S.; Phillips, H.; Geva, E.; Dunietz, B. D. *J. Am. Chem. Soc.* **2012**, *134*, 6944−7.
(66) Dick, B.; Hohlneicher, G. *J. Chem. Phys.* **1982**, *76*, 5755−5760.
(67) Goodson, T. G. *Acc. Chem. Res.* **2005**, *38*, 99−107.
(68) Andrews, D. L.; Ghoul, W. A. *J. Chem. Phys.* **1981**, *75*, 530.
(69) Craig, D. P.; Thirunamachandran, T. *Molecular Quantum Electrodynamics: An Introduction to Radiation Interaction*; Academic Press: London, 1984; p 120.
(70) Holt, N. E.; Kennis, J. T. M.; Fleming, G. R. *J. Chem. Phys.* **2004**, *108*, 19029−19035.
(71) Ceroni, P.; Balzani, V. *J. Phys. Chem. B* **2012**, *78*, 21−39.
(72) Langhals, H.; Esterbauer, A. J.; Walter, A.; Riedle, E.; Pugliesi, I. *J. Am. Chem. Soc.* **2010**, 16777−16782.
(73) Kleiman, V. *J. Phys. Chem. B* **2001**, *105*, 5595−5598.
(74) Ito, A.; Stewart, D. J.; Knight, T. E.; Fang, Z.; Brennaman, M. K.; Meyer, T. J. *J. Phys. Chem. B* **2013**, *117*, 3428−3438.
(75) Varnavski, O. P.; Ostrowski, J. C.; Sukhomlinova, L.; Twieg, R. J.; Bazan, G. C.; Goodson, T. *J. Am. Chem. Soc.* **2002**, *124*, 1736−43.
(76) Varnavski, O.; Leanov, a.; Liu, L.; Takacs, J.; Goodson, T. *Phys. Rev. B* **2000**, *61*, 12732−12738.
(77) Loura, L. M. S. *Int. J. Mol. Sci.* **2012**, *13*, 15252−70.
(78) Albrecht, C.; Lakowicz, J. *Anal. Bioanal. Chem.* **2008**, *390*, 1223−1224.
(79) Kusba, J.; Lakowicz, J. *J. Chem. Phys.* **1999**, *111*, 89−99.
(80) Jablonski, A. *Bull. Acad. Pol. Sci. Ser A* **1960**, *8*, 259−264.
(81) Baumann, J.; Fayer, M. D. *J. Chem. Phys.* **1986**, *85*, 4087−4107.
(82) Jablonski, A. *Acta Phys. Pol., A* **1970**, *38*, 453−458.
(83) Van Der Meer, B. W.; Coker, G., III; Chen, S.-Y. *Resonance Energy Transfer Theory and Data*; Wiley-VCH: New York, 1991.

NOTE ADDED AFTER ASAP PUBLICATION

Figure 7 was incorrect in the version published ASAP August 9, 2013; the correct version reposted August 12, 2013.